© 2021. Published by The Company of Biologists Ltd | Journal of Experimental Biology (2021) 224, jeb230607. doi:10.1242/jeb.230607

RESEARCH ARTICLE

Testing the influence of crushing surface variation on seed-cracking performance among beak morphs of the African seedcracker *Pyrenestes ostrinus*

Nicola S. Heckeberg[1,2,*], Philip S. L. Anderson[3] and Emily J. Rayfield[2]

ABSTRACT

Extreme phenotypic polymorphism is an oft-cited example of evolutionary theory in practice. Although these morphological variations are assumed to be adaptive, few studies have biomechanically tested such hypotheses. *Pyrenestes ostrinus* (the African seedcracker finch) shows an intraspecific polymorphism in beak size and shape that is entirely diet driven and allelically determined. Three distinct morphs feed upon soft sedge seeds during times of abundance, but during lean times switch to specializing on three different species of sedge seeds that differ significantly in hardness. Here, we test the hypothesis that beak morphology is directly related to consuming seeds of different hardness. We used a novel experimental analysis to test how beak morphology affects the efficiency of cracking sedge seeds of variable hardness, observing that neither mandibular ramus width nor crushing surface morphology had significant effects on the ability to crack different seed types. It is likely that feeding performance is correlated with other aspects of beak size and shape, such as beak depth and strength, muscle force or gape. Our results highlight how even seemingly straightforward examples of adaptive selection in nature can be complex in practice.

KEY WORDS: Bite force, Disruptive selection, Estrildidae, Feeding, Polymorphism, Seedcracker

INTRODUCTION

The African seedcracker *Pyrenestes ostrinus* (Estrildidae; Fig. 1) is distributed across West and Central Africa, an area with a tropical continental climate and little variability in the annual rainfall (Smith, 1987; Smith et al., 2001). It is well known as a classic polymorphic taxon, for which beak size and shape vary across three distinct yet interbreeding morphs produced by a single diallelic locus (Grant, 1986; Smith, 1987, 1993; Slabbekoorn and Smith, 2000; von Holdt et al., 2018). The three morphs vary primarily in mandible width, and are referred to as small (<14 mm), large (14–17.5 mm) and mega (>17.5 mm) (Fig. 1; Grant, 1986; Slabbekoorn and Smith, 2000; Smith et al., 2001). The coefficient of variation of the bill size is at least as large as in Darwin's finches, in which the variation is mainly referred to distinct species (Smith, 1987, 1993; Delaney et al., 2005). Unlike other polymorphic avian species, the *Pyrenestes* polymorphism is completely independent of geographic origin (Smith, 1987, 1993; Grant and Grant, 2002), sex (Smith et al., 2001), size (Grant and Grant, 2002) and age (Smith, 1997).

A recent genetic study (von Holdt et al., 2018) demonstrated that the differences in beak size between the small and large morphs can be explained by a simple genetic step, while the transition to the mega morph is likely driven by more complex controls. By contrast, in Darwin's finches, hundreds of loci are involved in maintaining their phenotypic diversity (Lawson and Petren, 2017).

The diet of *P. ostrinus* consists largely of three types of sedge seeds of varying hardness: soft (*Scleria goossensii*), hard (*Scleria verrucosa*) and very hard (*Scleria racemosa*) (Fig. 2; Clabaut et al., 2009). When the seeds are abundant, all morphs prefer the small, soft seeds, which are easiest to crack and therefore offer the most gain for least effort (Smith and Skúlason, 1996; Smith et al., 2001). During times of food scarcity, the large and mega morphs specialize on the hard and very hard seeds, respectively (Fig. 2B,C), whereas the small morphs adapt to a more generalist feeding habit including other grass seeds (Smith, 1997).

Pyrenestes' polymorphism may be related to the different *Scleria*-based diets altering feeding performance (Skúlason and Smith, 1995; Smith and Skúlason, 1996; Slabbekoorn and Smith, 2000). The inferred ecological hypothesis is that the larger morphs are able to crack the harder seeds more efficiently than can the smaller morphs, which is driving the polymorphism.

Although previous analyses on food-processing structures often focused on mammalian groups, the basic principles can be generalized to any surface morphology used to crack stiff, resistant food items such as seeds (Benkman, 1987, 1988; van der Meij and Bout, 2000). The morphology of the surface used for food processing can have a strong effect on fracturing food (Evans and Sanson, 1998, 2003; Lucas, 2004; Ungar, 2004; Freeman and Lemen, 2006; Berthaume et al., 2010; Crofts and Summers, 2014; Kolmann et al., 2015). Several features characterize the surface morphology of the seedcracker beak, such as the size of the entire crushing area, as well as the width of the ridges and depth of depressions on the crushing surface. The constellation of ridges and depressions may also be important in fracture ability.

It is likely that the crushing surface morphology of the seedcracker beaks evolved specifically to resist fracture rather than for force application, the latter being the function of the jaw muscles (Clabaut et al., 2009). Therefore, the beak morphology is most likely optimized to simultaneously enhance force application to the seed while avoiding fracture in the beak by dissipating stress. Because the assumption that beak morphology predicts feeding ecology has rarely been quantified (Navalón et al., 2019), our aim was to assess whether the differences in width and morphology of the beaks' crushing surface seen in the three seedcracker morphs

[1]Museum für Naturkunde, Leibniz Institute for Evolution and Biodiversity Research, Invalidenstr. 43, 10115 Berlin, Germany. [2]School of Earth Sciences, University of Bristol, Life Sciences Building, 24 Tyndall Avenue, Bristol BS8 1TQ, UK. [3]Department of Evolution, Ecology and Behavior, University of Illinois, 515 Morrill Hall, 505 S. Goodwin Ave, Urbana, IL 61801, USA.

*Author for correspondence (nicola.heckeberg@smnk.de)

N.S.H., 0000-0001-6542-8719; P.S.L.A., 0000-0001-7133-8322; E.J.R., 0000-0002-2618-750X

Received 16 June 2020; Accepted 18 January 2021

Journal of Experimental Biology (2021) 224, jeb230607. doi:10.1242/jeb.230607

Fig. 1. *Pyrenestes ostrinus* and examples of the variation in beak sizes. (A) Adult male black-bellied seedcracker, Assouinde, Côte d'Ivoire, November 2017. Photograph by Lionel Sineux. (B) The three morphs of *P. ostrinus* – small, large and mega – in lateral view. (C) The three morphs of *P. ostrinus* in ventral view. Note the differences in mandible width. Scale bars: 1 cm.

affect the efficiency of the beak for cracking the three different seed types. We therefore tested the direct interaction between the crushing surface, seed type and the work (energy) involved in seed cracking, not the bite force itself.

Here, we performed a series of biomechanical fracture experiments on different seed varieties using tools that approximate the bony crushing surfaces of *Pyrenestes* beak morphs. We reasoned that the less energy it takes to crack the seeds, the less danger to the beaks' structural integrity. Furthermore, if beak surface morphology is related to feeding ability, we would expect morphological differences in crushing surfaces to affect the work (energy) required to fracture a seed. Specifically, we predicted that tools that resemble mega morph bill morphology should crush the mega seeds for a lower work expenditure than would tools that resemble the small and large morphs.

MATERIALS AND METHODS

Beaks

One skull of each of the three different morphs and accompanying computed tomography (CT) scan data of *Pyrenestes ostrinus* (Vieillot 1805) were available to scrutinize differences in beak shape and surface morphology (provided by Thomas B. Smith, UCLA, Los Angeles, CA, USA; small morph 4606, large morph 5617 and mega morph 5103). The mandibles were separated from the skulls by dissecting out the jaw muscles. The most obvious difference between the beaks is the size, which can be observed most clearly in total mandible width (Fig. 1, Fig. S1A, Table S1). The crushing surfaces of the mandibles differ in width and curvature in cross section. The widths of the crushing surface on the mandible were 2–3 mm in the small morph, 3–4 mm in the large morph and 4–5 mm in the mega morph (Table S1). The curvature variations were as follows: the small morph has a flat, horizontal crushing surface (Fig. 2A); the large morph has a slightly curved crushing surface, whereas the central part of the mandible is nearly flat and becomes more rounded towards the labial and lingual sides (Fig. 2B); in the mega morph, a strong curvature can be observed, whereas the most curved part is in the central part of the mandible forming a tip and becoming less strongly bent towards the labial and lingual sides (Fig. 2C). Measurements of different areas of the mandible were taken with a digital calliper with a resolution of 10 µm. A detailed description of the morphology is provided in Fig. S3 and its legend; measurements are shown in Table S1.

Gape

To consider whether it would still be possible for the jaw muscles to apply close to maximal bite force, the distance between the tip of the upper and the lower beak (gape) was measured with a digital calliper while placing each seed type, one at a time, between the beaks at the place where they are cracked. This was done after the dissection of the jaw muscles, but with the jaw joints in contact with each other. The seed, the lower beak and the upper beak were held with one hand, and the gape was measured with the other hand. This procedure visualized how wide each of the beaks have to be opened to hold each seed type.

Seeds

Samples of *S. goossensii*, *S. verrucosa* (from Ndibi, Cameroon) and *S. racemosa* (from Wakwa, Cameroon) were collected by

Journal of Experimental Biology (2021) 224, jeb230607. doi:10.1242/jeb.230607

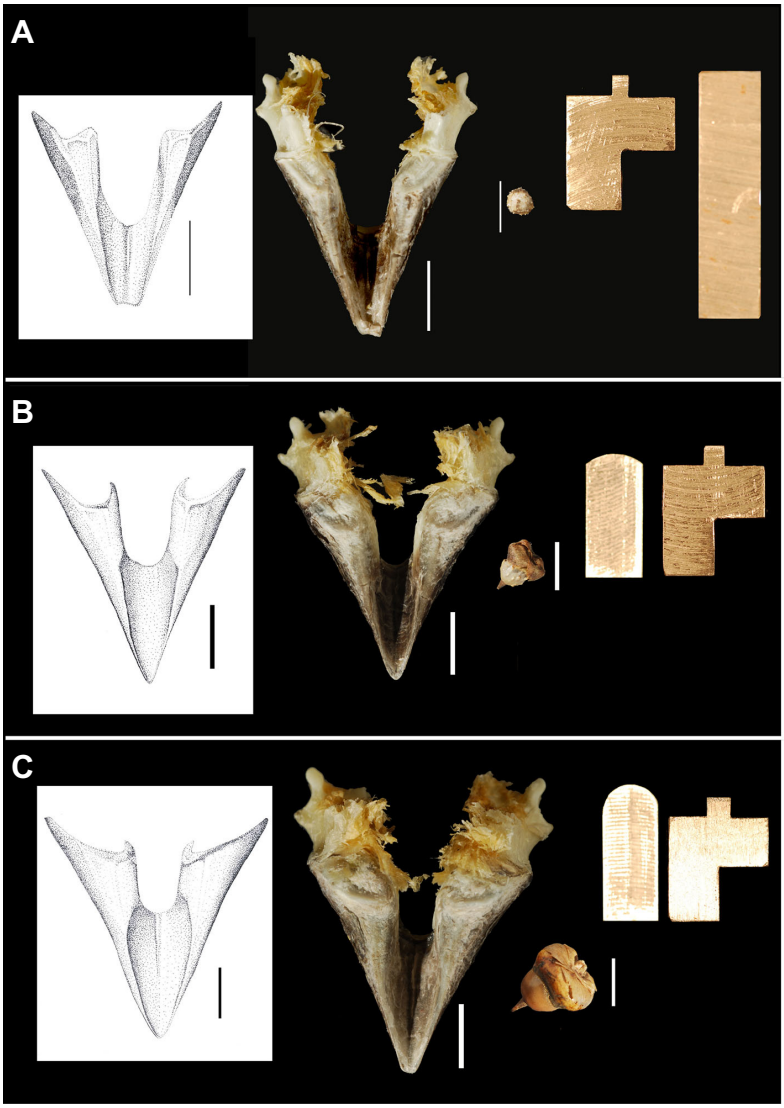

Fig. 2. Overview of the mandible morphology, *Scleria* seed type and respective tools for the three different morphs of *P. ostrinus*. (A) Small morph mandible with 3 mm ridge tool and flat upper blade, with *Scleria goossensii* seed. (B) Large morph mandible with 4 mm ridge tool and weakly curved upper blade, with *Scleria verrucosa* seed. (C) Mega morph mandible with 5 mm ridge tool and curved upper blade, with *Scleria racemosa* seed. All mandibles in dorsal view. Scale bars: 1 cm (beaks), 0.5 cm (seeds). See Fig. S3 and its legend for further details on beak morphology.

T. B. Smith ∼10–20 years ago. The three types of sedge seeds – *S. goossensii* (soft), *S. verrucosa* (hard) and *S. racemosa* (very hard) – are easy to distinguish by their size and morphology (Fig. 2). *Scleria goossensii* has a soft pericarp with a rough surface and tiny spikes. The mean diameter is 2.226 mm (N=12), and the cupule is only one-third of the seed size. Crushing the soft seed, the pericarp usually stayed in one piece and only burst open at one spot. The hardness is ∼13 N (Clabaut et al., 2009). *Scleria verrucosa* has a rough pericarp surface with remarkable thorns and spikes. The cupule is nearly as large as the whole seed. These hard seeds have a mean diameter of 2.878 mm (N=12), crushed in a brittle manner and have a hardness of ∼153 N (Clabaut et al., 2009). *Scleria racemosa* has a smooth, shiny pericarp with a cupule, which is nearly as large as the seed. The mean diameter is 4.850 mm (N=12). They also crushed in a brittle manner and have a hardness of ∼299 N (Clabaut et al., 2009).

Mechanical testing

The experiments were undertaken with a custom testing device, originally developed as a double-bladed guillotine (Anderson and LaBarbera, 2008; Anderson, 2009; Anderson and Rayfield, 2012; Fig. S1C) that combines aspects of a single-blade guillotine (Atkins and Mai, 1979; Veland and Torrissen, 1999) and the scissors tests (Atkins and Mai, 1979; Pereira et al., 1997; Lucas, 2004; Anderson, 2009). This device allows for testing materials to be compressed between two custom-designed tools aligned against each other. Although previous work used custom-designed blades for tools, we used tools designed according to beak morphology (described below). One tool is set on an upper moveable platform, which is attached to a large screw (20 mm diameter, 3 mm pitch; SKF, Göteborg, Sweden) anchored to the base box. The counterpart tool is mounted on a force transducer (LC703-100; Omegadyne, Sunbury, OH, USA) that is attached to the box, but can be moved forwards, backwards and in lateral directions to ensure a precise alignment between the upper and lower tools. The force transducer measures the force needed to crack the seeds (in eV). Displacement differences between the upper platform and the box were measured (in mm) with a linear displacement sensor (HS50 Linear Displacement Sensor LDS; Vishay Measurements Group UK Ltd, Basingstoke, UK), which is attached to the side of the machine. An AC induction motor (SD18M; Parvalux, Bournemouth, UK; including a gearbox) moves the upper platform up and down with a constant velocity (1.9 mm s^{-1} by default) by rotating the screw. The part where the tools were mounted on the upper platform had to be stable and fixed to avoid tilting while cracking the seeds. Objects to be fractured are placed in the middle of the two tools (Anderson, 2009).

Journal of Experimental Biology (2021) 224, jeb230607. doi:10.1242/jeb.230607

Tools

Two different sets of tools were made of high-quality tool steel (RS Components, Corby, UK) to represent two different aspects of the crushing surfaces of the mandible in *Pyrenestes* morphs; one set varying in width (2 mm, 3 mm, 4 mm and 5 mm) and another set varying in curvature (flat, weak curvature, strong curvature; Fig. 2). The specific curvature of this latter set was based on curvature measured from CT scan images provided by Annelies Genbrugge (Ghent University, Ghent, Belgium). Each of these tools was paired with an upper flat tool in the double guillotine. This is a reasonable simplification for the curvature tests, as the upper beaks are not curved in the same way as the mandibular surfaces (see Figs S1–S4 and Table S1). The material properties of steel tools differ from those of the beaks' keratinous sheaths; therefore, there will be differences in stiffness, i.e. the steel tools are expected to be more robust and rigid than the beaks.

In addition, we ran a series of experiments with a three-point bending tool, which has two triangular ridges with a V-shaped dent between them on the lower platform opposed by a single V-shaped ridge on the upper platform. The ridge and groove morphology of the beaks' crushing surfaces indicates that this might be applicable in cracking the seeds (see Fig. S1B). With this set-up, we tested whether tools resembling a pestle-and-mortar structure (Lucas, 2004) provide different results than the more simplified tools above.

Data acquisition

Before every run, the force transducer and the displacement sensor had to be re-calibrated and zeroed, as the start height of the upper platform was different every time and to avoid biases from the force transducer. It was ensured that the linear displacement sensor touched the box. Seeds to be fractured were placed between the two tools, recording started, and the motor moved down the upper platform. The machine was stopped immediately after cracking the seed, and recording was stopped. Seed remains were removed, and everything was reset to the starting position. The signals from the force transducer and the displacement sensor were detected and amplified by a scanner (Vishay, 5000 series 5100B), and converted into force and displacement. The conversion is based on factory-set calibrations of the sensors (Anderson, 2009).

Each tool was tested on the three different types of seeds. As the seeds are a natural product, there is variability in their physical properties. Therefore, each tool–seed combination was tested 12 times to obtain a statistical mean. The peak force values (in N) of each run were also collected to compare the forces required to crack the seeds.

Data analyses

Data collected by the scanner were exported to Excel as displacement (in mm and mV/V) and force (in calibrated values N and mV). Only the values for displacement in mm and force in N were used for further processing. First, a force-displacement curve was plotted, then a start and end point for the calculations were determined, and the area under this curve was calculated using the following formula:

$$I = 0.5 \times (x_2 - x_1) \times |F_2 - F_1| + (x_2 - x_1) \times F_1, \quad (1)$$

where I is the area under the curve between two points (integral), x is displacement and F is force.

As the area under the curve is equal to the work done, the work value is the sum of the integral (I) values from the start to the end point (Fig. S2). The work values are important for comparisons of the effectiveness of the different set-ups, because the work represents how much energy it takes to break the seeds. This again is important, as it is in an organism's interest to maximize net energy gain (energy in food item minus energy cost of food acquisition). Hence, energy is used in comparisons between the different morphs.

We performed a two-way ANOVA, including a *post hoc* Tukey's honestly significant difference test, on the work values of each seed–tool combination using R (https://www.R-project.org/). The categorical variable 'seed' had five levels (soft, $hard_1$, hard, $hard_2$, very hard) and the categorical variable 'tool' had eight levels (2 mm, 3 mm, 4 mm, 5 mm, flat, weak curvature, strong curvature, three-point bending).

RESULTS

Regardless of the tool used, the work required to crack the three different types of seeds differed by about one order of magnitude (Table 1, Fig. 3). Differences in cracking behaviour were also observed during the experiments: soft seeds were compressed flat, whereas hard and very hard seeds generally broke into multiple pieces. A subset of the hard seeds, *S. verrucosa*, fractured in a manner similar to the soft seeds at intermediate forces between the harder *S. verrucosa* seeds and the softer *S. goossensii* seeds (see Tables S2–S4 for details). Thus, it was possible to identify two different types of hard seeds: $hard_1$ and $hard_2$.

Each seed–tool combination was tested 12 times; because of the bimodal split of the hard seeds, sample sizes for the $hard_1$ and $hard_2$ seeds were smaller than 12 in most cases, according to our observations and the bimodal distribution of the values. The mean work value for *S. goossensii* was ∼0.0030 J. Work values ranged from 0.0105 J to 0.0296 J in the $hard_1$ seeds and from 0.0451 J to

Table 1. Mean work values for the different combinations of tool and *Scleria* seed types

	Work to fracture *Scleria* seed type (J)									
Tool type	*S. goossensii* (soft)	*N*	*S. verrucosa* ($hard_1$)	*N*	*S. verrucosa* (hard)	*N*	*S. verrucosa* ($hard_2$)	*N*	*S. racemosa* (very hard)	*N*
Flat	**0.00303**	12	0.02337	4	0.04470	12	0.08737	8	0.27542	11
Weak curvature	0.00281	9	**0.01635**	8	**0.04066**	12	**0.08928**	4	0.23202	11
Strong curvature	0.00273	12	0.02961	8	0.04753	12	0.08337	4	**0.22781**	9
2 mm	**0.00343**	12	0.02176	6	0.04861	12	0.07547	6	0.22678	12
3 mm	**0.00297**	12	**0.02243**	4	**0.05144**	12	**0.06594**	8	0.21781	10
4 mm	0.00330	12	**0.01838**	6	**0.05140**	12	**0.08441**	6	**0.26650**	11
5 mm	0.00332	11	0.01590	3	0.05524	12	0.06836	9	**0.21607**	12
Three-point	0.00542	12	0.01703	5	0.03608	12	0.04969	7	0.17271	7

The first three rows describe the tool curvature variations, the next four rows describe the variations in mandibular ramus width, and the last row shows the values for the three-point bending tool. Values in bold show the tool–seed combination that was expected to be the most effective, i.e. which should have the lowest value. hard, $hard_1$+$hard_2$.

Journal of Experimental Biology (2021) 224, jeb230607. doi:10.1242/jeb.230607

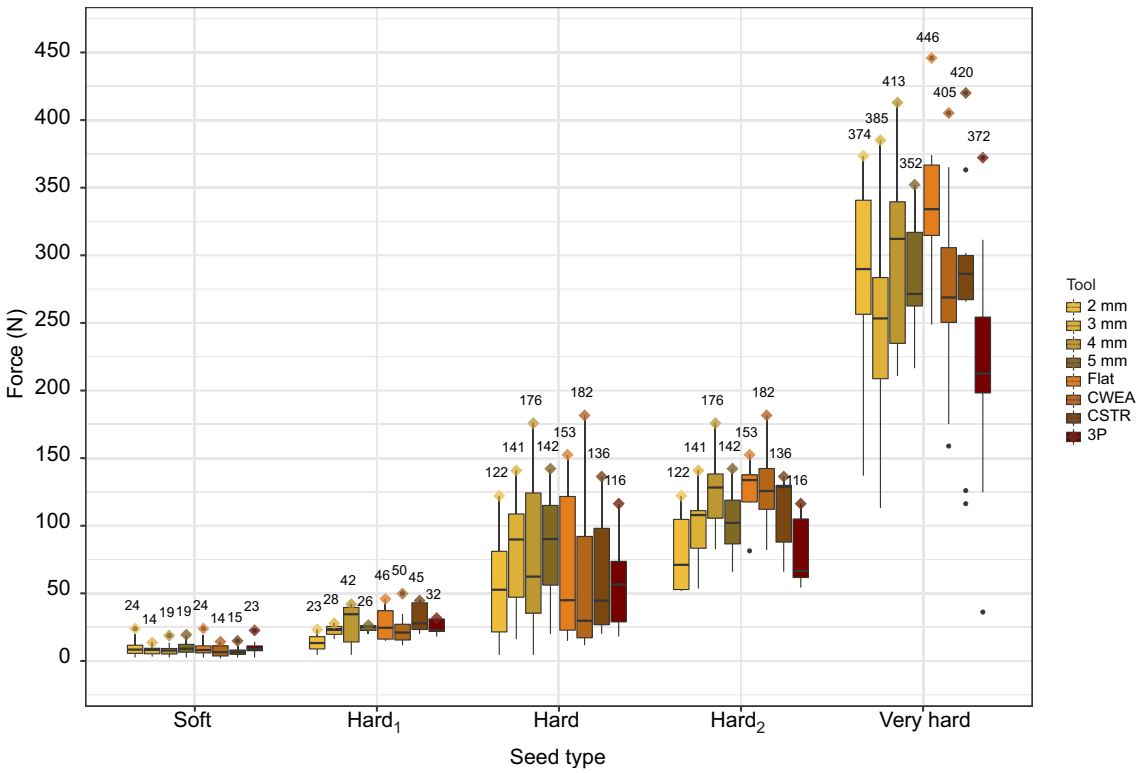

Fig. 3. Boxplot showing the force required to crack the different *Scleria* seed types with the different tools. Boxes represent the interquartile ranges (IQR) including the median. Whiskers represent the minimum and maximum ranges of the data with a distance of 1.5 times the IQR. The maximum force (in N) is indicated by the diamonds and values. Because the sample of hard seeds includes $hard_1$ and $hard_2$ samples, the maximum force values of hard and $hard_2$ seeds are equal. Note the low force values for the three-point bending tool combined with the $hard_2$ and very hard seeds. hard, $hard_1$+$hard_2$; CWEA, weak curvature; CSTR, strong curvature; 3P, three-point bending.

0.0893 J in the $hard_2$ seeds. For *S. racemosa*, the work values were between 0.1727 J and 0.2754 J (Table 1; Table S3). The highest measured peak force value was 445.89 N (*S. racemosa*). The mean peak force values for *S. goossensii* were between 7.0 N and 10.0 N. For *S. verrucosa* ($hard_1$), they ranged from 23.91 N to 34.07 N; for *S. verrucosa* ($hard_2$), they ranged from 91.51 N to 128.76 N; and for *S. racemosa*, they were between 218.91 N and 313.69 N (Fig. 3; Table S2).

The two-way ANOVA revealed statistically significant difference in work by seed type ($F_{4,28}$=485.50; $P \ll 0.001$) and less significant difference in work by tool type ($F_{7,28}$=2.39; P=0.02). The interaction between seed and tool type was not significant. The degrees of freedom of the residuals is 330. The *post hoc* Tukey test showed a significant pairwise difference between almost all seed–seed combinations ($P \ll 0.05$); for the $hard_1$–hard and hard–$hard_2$ combinations, the amount of variation was significant, but with larger P-values (P=0.001), and for the soft–$hard_1$ combination, the amount of variation was not significant (P=0.06). The pairwise difference of all tool–tool combinations was not significant ($P > 0.05$), except for the 4 mm–three-point (P=0.02) and the flat–three-point (P=0.01) combinations. The complete results of the ANOVA including P-values of the interaction between seed and tool types are provided in Dataset 1.

Thus, regardless of the seed type tested, there were no remarkable differences in work to fracture using tools based on the different crushing surface morphologies. Neither tools mimicking differences in surface width nor curvature had significant impact on the work values calculated (Table 1). Thus, the tools representing different crushing surface morphologies had no differentiated effect on seed-cracking efficiency.

The three-point bending tool had the lowest energy for the very hard seeds and the $hard_2$ seeds but was less economical for the soft and $hard_1$ seeds (Table 1), which might be caused by the smaller seeds fitting between the triangular ridges and, thus, having a lateral restriction rather than a three-point bending set-up.

Gape

For the small morph, the gape was negligible with the soft seed, 4 mm with the hard seed and 9–10 mm with the very hard seed. The large morph showed a negligible gape with the soft seed; a gape of 3.5 mm with the hard seeds, which also fit between the upper and lower beak without wobbling; and a gape of 9.5 mm with the very hard seed, which also fit between the beaks (without the cupule). For the mega morph, there was a negligible gape with the soft seed, a gape of 2–3 mm with the hard seed and a gape of 8.5 mm with the very hard seed. The very hard seed did not fit as well between the upper and lower beaks of the mega morph as the hard seed did between the upper and lower beaks of the large morph.

Crushing properties of the seeds

Scleria goossensii smashed easily without much resistance. For *S. verrucosa*, we observed that the hard seeds could be divided into two types of seeds. One type ($hard_2$) cracked with an audible noise and resistance; the other type ($hard_1$) smashed rather than cracked, showing very little resistance. Differences in the mean work value between the two types are significant for all tool pairings (ANOVA, $P \ll 0.05$). The reason for this observation is not evident; it could not be predicted from external morphology whether the seed will crack or smash. Both types of hard seeds always had intact fruits; hence, degeneration of the seeds is not the reason (Fig. S4). *Scleria*

racemosa showed either cracking or crushing behaviour accompanied by a loud cracking noise and strong resistance (Fig. S4). Nonetheless, in some of the very hard seeds, very little resistance was observed. These seeds contained dust inside instead of a proper fruit and were white on the outside instead of brown; hence, it was predicable whether a seed would show resistance. It is very likely that the white, very hard seeds were poorly preserved, and thus these seeds were excluded from the analyses. Even though poorly preserved seeds could be identified in most cases, there is still some possibility that intact seeds might behave slightly differently compared with the aged seeds used in this study.

Conducting the experiments with the three-point bending tool, the very hard seeds were divided into two half spheres, preserving the fruit as a whole (Fig. S4). With all other tools the very hard seeds and their fruits were crushed or cracked, respectively.

DISCUSSION

Our experimental results fail to support the hypothesis that variations in the width and morphology of the crushing surfaces of the mandibles in *P. ostrinus* will have an influence on seed-cracking efficiency. The crushing surface morphology of the mega morphs is no more efficient at cracking the hardest seeds than the crushing surface morphology of the small morphs. By focusing on the crushing surfaces, we isolate morphology that is closely associated with seed reduction. However, the morphological variation of the crushing surfaces we observed appears to have little influence on this presumed function. Given that the polymorphism is apparently tied to feeding and resource acquisition (Smith, 1987, 1997; Navalón et al., 2019), we propose that other morphological, biomechanical or genetic mechanisms may be responsible for triggering and maintaining the polymorphism expressed on the food-processing surface of the mandible.

For the three-point bending tool, the work-to-fracture values were lower when cracking the $hard_2$ and very hard seeds, in the same range for the $hard_1$ and hard seeds, and higher for the soft seeds, compared with the values obtained with the other tool types (Table 1). The three-point bending tool was built to create the three-point bending effect on the very hard seeds, which fit on top of the triangular ridges of the tool. The soft seeds, however, fit between those ridges, creating a lateral restriction, which probably explains the higher work values, because the two tools may have come into contact during the cracking. For the very hard and $hard_2$ seeds, crushing surfaces similar to those of the three-point bending tool seem to be advantageous. It is possible that the space between the upper and lower beak (when beaks are closed) resembles a three-point bending or pestle-and-mortar structure, at least for the mega morph and potentially for the large morph (Lucas, 2004). Also, the ridges on the mandible may be advantageous for initiating a crack in the seeds.

Although small beak tools can crack large seeds in our experimental setting, this does not mean that the smaller morphs possess the muscle mass required to generate such force. The relatively wide gape required for cracking the very hard seeds would be a challenge for certain birds, especially for the small and large morphs, but apparently possible for the mega morph; the size of large food particles eaten is correlated with gape width in some birds (Wheelwright, 1985). From our observations, it is questionable whether the small morph would be able to produce enough force to crack the very hard seeds with such a wide gape, as the adductor muscles might be too stretched to be contracted to effectively close the beak, and the angle between the force vectors might be too wide to take effect in cracking the seed. Furthermore, the properties of the keratinous beak are certainly also important, but the keratin sheath was not considered in our experiments. *In vivo* observations of the three morphs feeding on the three seed types would be helpful to support our findings.

Foraging efficiency is dependent on beak morphology; for example, beak depth influences bite force and deep beaks are crucial for husking hard seeds (Benkman, 1987). The beak morphology and size correspond to optima for times of limited food supply. The beak size and associated musculature also influence seed-husking ability and represent the upper limit for the largest and hardest seeds (Benkman, 1987, 1993). The optimal husking groove width of the palatine grooves of the keratinous beak are essential for securing seeds in the beak while seed husking (Benkman, 1987, 1993).

The individual husking technique of the finches should also be considered. Increased seed size makes husking and cracking more difficult; thus, the number of positioning movements before cracking increases with the size of the seed, and, therefore, seed husking time increases with seed size and hardness (Benkman, 1987; van der Meij et al., 2004). Large seeds are more difficult to position than small seeds, which affects the number of cracking attempts. There are also more cracking attempts when the size of the seed does not fit the husking grooves well, which may also result in a loss of the seed (van der Meij et al., 2004). The small morph, for example, would probably drop a seed that is too large or hard to crack rather than risk beak fracture in the cracking attempt. It should be noted that pre-cracked seeds might get picked up by another bird, and would then likely require fewer cracking attempts, because multiple cracking attempts lowers the strength of the seed husk (van der Meij et al., 2004). In this case, the force to eventually crack the seed, particularly the very hard seeds, might be slightly lower than gathered from our experiments (van der Meij et al., 2004).

A comparative study on finches and sparrows found that finches are capable of feeding on comparatively large/hard seeds in comparison to sparrows (Benkman and Pulliam, 1988). This means that sparrows have to intake more (small) seeds and finches are more vagile, covering large areas in search of seeds. Because small and large finches eat very different seed sizes, resource partitioning is more pronounced in finches than in sparrows, and the diets of small and large sparrows overlap (Benkman and Pulliam, 1988). This supports the observations in *P. ostrinus*.

Differences in size between morphs may also be correlated with the increased muscle mass in the skull necessary to crack harder seeds. In finches, beak dimensions and head width are correlated with bite force (van der Meij and Bout, 2004, 2006; Herrel et al., 2005a,b), which is dependent on the cross-sectional area of the jaw adductor muscles (Bowman, 1961; van der Meij and Bout, 2004, 2008). Similar relationships between beak size and bite force can be observed in *P. ostrinus*, but body size variations are independent of beak size variations (Grant and Grant, 2002). Finite element studies of mechanical stress in the beaks of Darwin's ground finches (Soons et al., 2010, 2012, 2015) suggest that beak morphologies evolve due to selection for avoidance of fractures and are optimized to resist natural loading. Thus, different beak shapes and crushing surface morphologies are ideal for mitigating risk of fracture with the species' preferred diet (Soons et al., 2015). Beak size in the large and mega morphs, which is independent of overall body size (Clabaut et al., 2009), may simply be to reinforce the beaks when cracking the much harder seeds.

It is likely that these three factors – beak size, muscle size and bite force – correlate with each other in the African seedcrackers,

promoting the different cracking forces/abilities. Size-independent factors such as the depression angle of the bill (van der Meij and Bout, 2008) can influence the bite force as well. A thick rhamphotheca, the keratinous sheath that surrounds the jaw bones and forms the actual beak, a strong downward inclination of the upper beak and a strongly developed jugal have been shown to be important features in increasing bite force (Bowman, 1961; van der Meij and Bout, 2008; Soons et al., 2012). It is possible that the differences in beak size between the *Pyrenestes* morphs are caused by differences in jaw musculature, which may reflect and influence differences in feeding performance between these morphs. Hence, soft tissues features, rather than the rhamphothecal morphology, may be driving selection and the maintenance of the polymorphism in African seedcracker finches.

Our results show that the relationship between the beaks' crushing surface width and curvature and feeding ecology is more complex than anticipated, which was also demonstrated in a study on modern birds (Navalón et al., 2019). However, Pigot et al. (2020) showed that the avian trophic diversity could be described by a traitspace using only four dimensions. Beak shape in seed eaters may be subject to selection to resist feeding forces and reduce fracturing (Soons et al., 2015); thus, understanding how beak polymorphisms evolve will help to explain the patterns of selection on beak size and shape in natural selection.

Acknowledgements
We thank M. Dury and A. Povey from the School of Earth Sciences workshop (University of Bristol) for constructing beak tools and S. Powell (University of Bristol) for photography. We thank A. Genbrugge, who provided the CT scans; T. B. Smith, who collected and sent the skulls of the birds and the seeds; and L. Sineux for the photograph of the finch. T. B. Smith and A. Herrel kindly provided helpful comments and discussion. We also thank D. Sustaita and one anonymous reviewer for their constructive comments on the manuscript.

Competing interests
The authors declare no competing or financial interests.

Author contributions
Conceptualization: N.S.H., P.S.L.A., E.J.R.; Methodology: N.S.H., P.S.L.A.; Formal analysis: N.S.H.; Investigation: N.S.H.; Resources: P.S.L.A., E.J.R.; Data curation: N.S.H.; Writing - original draft: N.S.H.; Writing - review & editing: N.S.H., P.S.L.A., E.J.R.; Visualization: N.S.H.; Supervision: P.S.L.A., E.J.R.; Project administration: P.S.L.A., E.J.R.

Funding
This research received no specific grant from any funding agency in the public, commercial or not-for-profit sectors.

Supplementary information
Supplementary information available online at
https://jeb.biologists.org/lookup/doi/10.1242/jeb.230607.supplemental

References
Anderson, P. S. L. (2009). The effects of trapping and blade angle of notched dentitions on fracture of biological tissues. *J. Exp. Biol.* **212**, 3627-3632. doi:10.1242/jeb.033712
Anderson, P. S. L. and LaBarbera, M. (2008). Functional consequences of tooth design: effects of blade shape on energetics of cutting. *J. Exp. Biol.* **211**, 3619-3626. doi:10.1242/jeb.020586
Anderson, P. S. L. and Rayfield, E. J. (2012). Virtual experiments, physical validation: Dental morphology at the intersection of experiment and theory. *J. R. Soc. Interface* **9**, 1846-1855. doi:10.1098/rsif.2012.0043
Atkins, A. G. and Mai, Y. W. (1979). On the guillotining of materials. *J. Mat. Sci.* **14**, 2747-2754. doi:10.1007/BF00610649
Benkman, C. (1987). Crossbill foraging behavior, bill structure, and patterns of food profitability. *Wilson Bull.* **99**, 351-368.
Benkman, C. W. (1988). Seed handling ability, bill structure, and the cost of specialization for crossbills. *Auk* **105**, 715-719. doi:10.1093/auk/105.4.715
Benkman, C. W. (1993). Adaptation to single resources and the evolution of crossbill (*Loxia*) diversity. *Ecol. Mono.* **63**, 305-325. doi:10.2307/2937103
Benkman, C. W. and Pulliam, H. R. (1988). The comparative feeding rates of North American sparrows and finches. *Ecology* **69**, 1195-1199. doi:10.2307/1941274
Berthaume, M., Grosse, I. R., Patel, N. D., Strait, D. S., Wood, S. and Richmond, B. G. (2010). The effect of early hominin occlusal morphology on the fracturing of hard food items. *Anat. Rec.* **293**, 594-606. doi:10.1002/ar.21130
Bowman, R. I. (1961). Morphological differentiation and adaptation in the Galapagos finches. *U. Calif. Publ. Zool.* **58**, 1-302.
Clabaut, C., Herrel, A., Sanger, T. J., Smith, T. B. and Abzhanova, A. (2009). Development of beak polymorphism in the African seedcracker, *Pyrenestes ostrinus*. *Evol. Dev.* **11**, 636-646. doi:10.1111/j.1525-142X.2009.00371.x
Crofts, S. B. and Summers, A. P. (2014). How to best smash a snail: the effect of tooth shape on crushing load. *J. R. Soc. Interface* **11**, 20131053. doi:10.1098/rsif.2013.1053
Delaney, K. S., Pires, D., Holder, K., Bardeleben, C. and Smith, T. B. (2005). Isolation of polymorphic tetranucleotide microsatellite markers for the black-bellied seedcracker (*Pyrenestes ostrinus*). *Mol. Ecol. Notes* **5**, 774-776. doi:10.1111/j.1471-8286.2005.01059.x
Evans, A. R. and Sanson, G. D. (1998). The effect of tooth shape on the break-down of insects. *J. Zool.* **246**, 391-400. doi:10.1111/j.1469-7998.1998.tb00171.x
Evans, A. R. and Sanson, G. D. (2003). The tooth of perfection: functional and spatial constraints on mammalian tooth shape. *Biol. J. Linn. Soc.* **78**, 173-191. doi:10.1046/j.1095-8312.2003.00146.x
Freeman, P. W. and Lemen, C. (2006). Puncturing ability of idealized canine teeth: edged and non-edged shanks. *J. Zool.* **269**, 51-56. doi:10.1111/j.1469-7998.2006.00049.x
Grant, P. R. (1986). *Ecology and Evolution of Darwin's Finches*. Princeton: University Press, Princeton.
Grant, P. R. and Grant, B. R. (2002). Unpredictable evolution in a 30-year study of Darwin's finches. *Science* **296**, 707-711. doi:10.1126/science.1070315
Herrel, A., Podos, J., Huber, S. K. and Hendry, A. P. (2005a). Evolution of bite force in Darwin's finches: a key role for head width. *J. Evol. Biol.* **18**, 669-675. doi:10.1111/j.1420-9101.2004.00857.x
Herrel, A., Podos, J., Huber, S. K. and Hendry, A. P. (2005b). Bite performance and morphology in a population of Darwin's finches: implications for the evolution of beak shape. *Funct. Ecol.* **19**, 43-48. doi:10.1111/j.0269-8463.2005.00923.x
Kolmann, M. A., Crofts, S. B., Dean, M. N., Summers, A. P. and Lovejoy, N. R. (2015). Morphology does not predict performance: jaw curvature and prey crushing in durophagous stingrays. *J. Exp. Biol.* **218**, 3941-3949. doi:10.1242/jeb.127340
Lawson, L. P. and Petren, K. (2017). The adaptive genomic landscape of beak morphology in Darwin's finches. *Mol. Ecol.* **26**, 4978-4989. doi:10.1111/mec.14166
Lucas, P. W. (2004). *Dental Functional Morphology: How Teeth Work*. Cambridge: Cambridge University Press.
Navalón, G., Bright, J. A., Marugán-Lobón, J. and Rayfield, E. J. (2019). The evolutionary relationship among beak shape, mechanical advantage, and feeding ecology in modern birds. *Evolution* **73**, 422-435. doi:10.1111/evo.13655
Pereira, B. P., Lucas, P. W. and Swee-Hin, T. (1997). Ranking the fracture toughness of thin mammalian soft tissues using scissors cutting test. *J. Biomech.* **30**, 91-94. doi:10.1016/S0021-9290(96)00101-7
Pigot, A. L., Sheard, C., Miller, E. T., Bregman, T. P., Freeman, B. G., Roll, U., Seddon, N., Trisos, C. H., Weeks, B. C. and Tobias, J. A. (2020). Macroevolutionary convergence connects morphological form to ecological function in birds. *Nature Ecol. Evol.* **4**, 230-239. doi:10.1038/s41559-019-1070-4
Skúlason, S. and Smith, T. B. (1995). Resource polymorphisms in vertebrates. *Trends Ecol. Evol.* **10**, 366-370. doi:10.1016/S0169-5347(00)89135-1
Slabbekoorn, H. and Smith, T. B. (2000). Does bill size polymorphism affect courtship song characteristics in the African finch *Pyrenestes ostrinus*? *Biol. J. Linn. Soc.* **71**, 737-753. doi:10.1111/j.1095-8312.2000.tb01288.x
Smith, T. B. (1987). Bill size polymorphism and intraspecific niche utilization in an African finch. *Nature* **329**, 717-719. doi:10.1038/329717a0
Smith, T. B. (1993). Disruptive selection and genetic basis of bill size polymorphism in the African finch *Pyrenestes*. *Nature* **363**, 618-620. doi:10.1038/363618a0
Smith, T. B. (1997). Adaptive significance of the mega-billed form in the polymorphic Black-bellied Seedcracker *Pyrenestes ostrinus*. *Ibis* **139**, 382-387. doi:10.1111/j.1474-919X.1997.tb04638.x
Smith, T. B. and Skúlason, S. (1996). Evolutionary significance of resource polymorphisms in fishes, amphibians, and birds. *Annu. Rev. Ecol. Syst.* **27**, 111-133. doi:10.1146/annurev.ecolsys.27.1.111
Smith, T. B., Schneider, C. J. and Holder, K. (2001). Refugial isolation versus ecological gradients. *Genetica* **112-113**, 383-398. doi:10.1023/A:1013312510860
Soons, J., Herrel, A., Genbrugge, A., Aerts, P., Podos, J., Adriaens, D., de Witte, Y., Jacobs, P. and Dirckx, J. (2010). Mechanical stress, fracture risk and beak evolution in Darwin's ground finches (*Geospiza*). *Phil. Trans. R. Soc. B* **365**, 1093-1098. doi:10.1098/rstb.2009.0280
Soons, J., Herrel, A., Genbrugge, A., Adriaens, D., Aerts, P. and Dirckx, J. (2012). Multi-layered bird beaks: a finite-element approach towards the role of keratin in stress dissipation. *J. R. Soc. Interface* **9**, 1787-1796. doi:10.1098/rsif.2011.0910

Soons, J., Genbrugge, A., Podos, J., Adriaens, D., Aerts, P., Dirckx, J. and Herrel, A. (2015). Is beak morphology in Darwin's finches tuned to loading demands? *PLoS ONE* **10**, e0129479. doi:10.1371/journal.pone.0129479

Ungar, P. (2004). Dental topography and diets of *Australopithecus afarensis* and early *Homo*. *J. Hum. Evol.* **46**, 605-622. doi:10.1016/j.jhevol.2004.03.004

van der Meij, M. A. A. and Bout, R. G. (2000). Seed selection in the Java sparrow (*Padda oryzivora*): preference and mechanical constraint. *Can. J. Zool.* **78**, 1668-1673. doi:10.1139/z00-114

van der Meij, M. A. A. and Bout, R. G. (2004). Scaling of jaw muscle size and maximal bite force in finches. *J. Exp. Biol.* **207**, 2745-2753. doi:10.1242/jeb.01091

van der Meij, M. A. A. and Bout, R. G. (2006). Seed husking time and maximal bite force in finches. *J. Exp. Biol.* **209**, 3329-3335. doi:10.1242/jeb.02379

van der Meij, M. A. A. and Bout, R. G. (2008). The relationship between shape of the skull and bite force in finches. *J. Exp. Biol.* **211**, 1668-1680. doi:10.1242/jeb.015289

van der Meij, M. A. A., Griekspoor, M. and Bout, R. G. (2004). The effect of seed hardness on husking time in finches. *Anim. Biol.* **54**, 195-205. doi:10.1163/1570756041445164

Veland, J. O. and Torrissen, O. J. (1999). The texture of Atlantic salmon (*Salmo salar*) muscle as measured instrumentally using TPA and Warner-Brazler shear test. *J. Sci. Food Agr.* **79**, 1737-1746. doi:10.1002/(SICI)1097-0010(199909)79:12<1737::AID-JSFA432>3.0.CO;2-Y

von Holdt, B. M., Kartzinel, R. Y., Huber, C. D., Le Underwood, V., Zhen, Y., Ruegg, K., Lohmueller, K. E. and Smith, T. B. (2018). Growth factor gene IGF1 is associated with bill size in the black-bellied seedcracker *Pyrenestes ostrinus*. *Nat. Commun.* **9**, 1-12. doi:10.1038/s41467-017-02088-w

Wheelwright, N. T. (1985). Fruit-size, gape width, and the diets of fruit-eating birds. *Ecology* **66**, 808-818. doi:10.2307/1940542

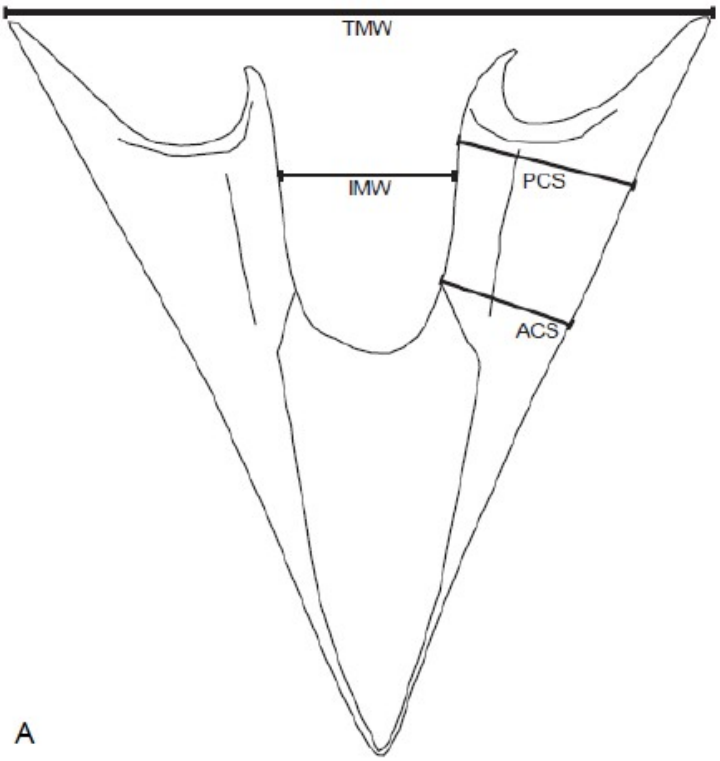

A

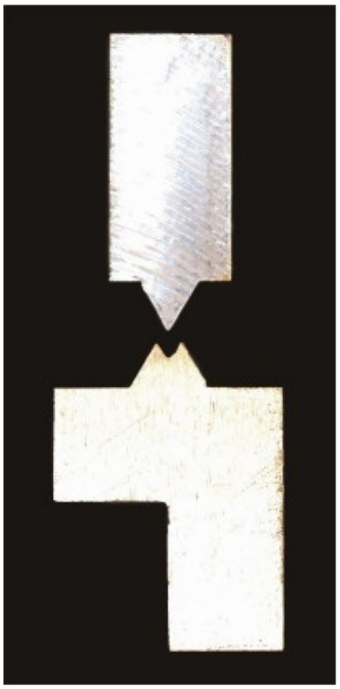

B

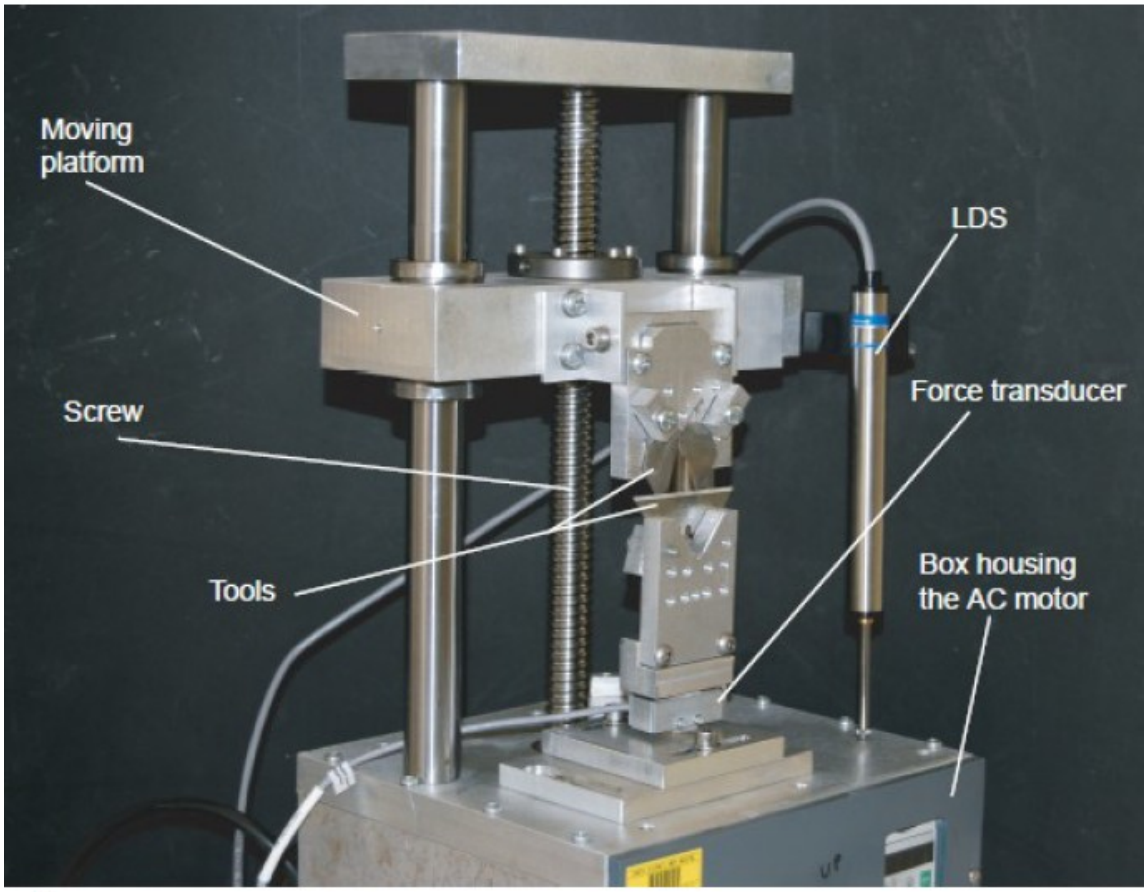

C

Figure S1. (A) Schematic drawing of the mandible showing where the measurements were" taken (Table S1). TMW = total mandible width, IMW = inner mandible width, ACS =" anterior crushing surface width, PCS = posterior crushing surface width. (B)Three-point" bending set-up created for the very hard seed size, but it was tested with each seed type.
(C)"Double guillotine testing device. Physical testing device with tools (blades in this case)" mounted on the force transducer (which measures the force during experiments), and on the" moveable upper platform. On the right the linear displacement sensor (LDS) measures the" distance the upper platform covers during experiments. The box houses the AC induction" motor, which rotates the screw in order to move the upper platform.

Force [N]	Displacement [mm]	Force corrected		
0.6462	0.7892	-0.6462		
0.6462	0.92	-0.6462	Calculation of the area beneath the curve (= work) according to the equation in the main text.	
0.6462	1.0635	-0.6462		
0.6462	1.1985	-0.6462		
1.9387	1.3504	-1.9387	=(0.5*(B6-B5)*(ABS(C6-C5))+(B6-B5)*C5)	
0	1.4855	0	-0.1310	**Start**
-3.2311	1.6121	3.2311	0.2045	
-40.0658	1.7218	40.0658	2.3748	
-85.9476	1.7809	85.9476	3.7237	
-118.9049	1.7851	118.9049	0.4302	
-160.9094	1.8189	160.9094	4.7289	
-209.3761	1.8569	209.3761	7.0354	
-169.3103	1.9581	169.3103	23.2162	
0.6462	2.359	-0.6462	101.9443	**End**
-1.9387	2.5068	1.9387	143.5270	**Work [N*mm]**
-2.5849	2.5785	2.5849	0.1435	**Work [J]**
-0.6462	2.5827	0.6462		
-1.2924	2.5827	1.2924		
-0.6462	2.5827	0.6462		

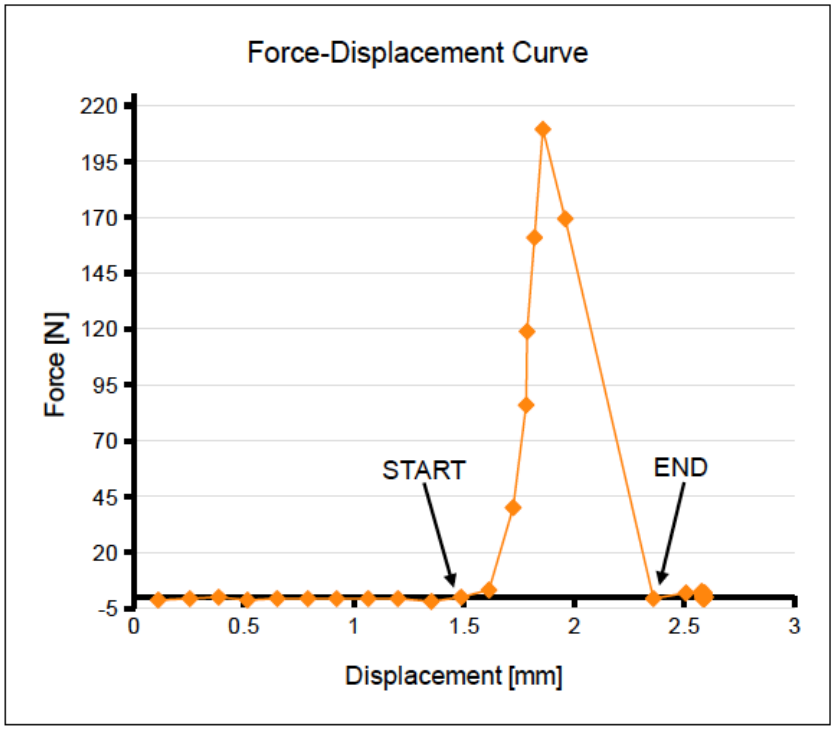

Figure S2. Example for the work value calculation. The diagram shows the area for the integral calculus to get the work value. The area of individual slices between two adjacent data points, the x axis and the curve were calculated, and the work values of the individual slices were added. The start and end points are determined by the last and first data points with $x \approx 0$.

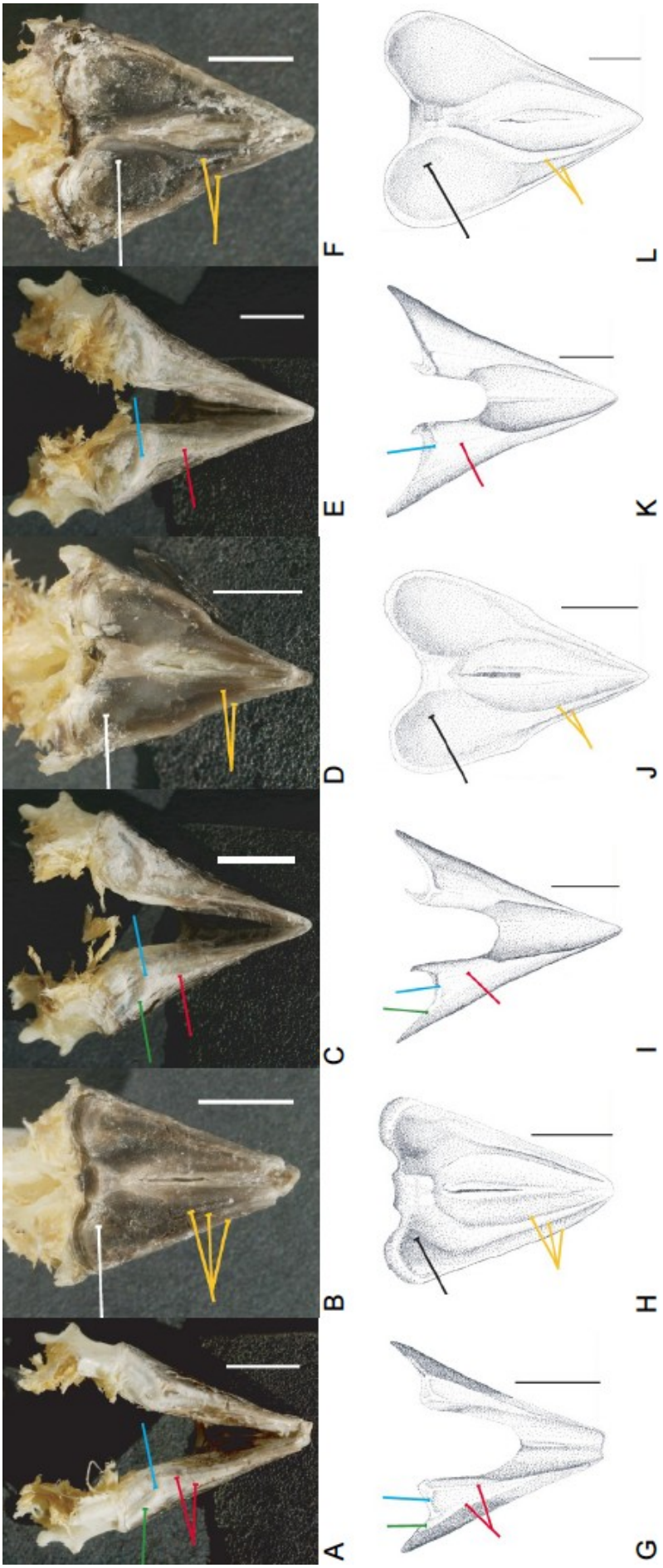

Figure S3. Beak morphology. The upper beaks show more morphological differences than the mandible. The mandibles have grooves and ridges in the anterior part, which are probably used to avoid a shearing or torsion of the two beaks against each other. The posterior part shows slight differences in presence or absence of ridges and the grade of roundness (flat, weak curve, strong curvature). A trend in the mandible is that the side-to-side ridges become longer and better developed the larger the beak. The upper beaks show variations in the dimensions of depressions and ridges. These ridges are further apart the larger the morph. The depressions in the posterior part of the beak are the most variable. In the small morph the depression is narrow and deep. It is shallower, more flattened and wider in the large and the mega morph.

(A, B, G, H) Crushing surface morphology of the small morph. (A, G) Mandible. There is one ridge, which runs on the lingual side from the tip of the beak to the posterior end. After about 5 mm from the tip another ridge originates from the lingual ridge under an angle of less than 20° that runs on the labial side to the posterior end of the mandible. These two anterior-posterior ridges (red arrows) are connected at their posterior ends with another ridge, which runs more or less in the lingual-labial direction, forming a triangle. The width of the side-to-side ridge (blue arrow) is 2-3 mm. The area between these three ridges forms a shallow depression. There are another two short ridges each originating from the posterior edges of the triangle one in the lingual direction and the other one in the labial direction (green arrow). These two ridges probably do not play a role in the cracking process, but may be useful for resisting forces or stabilising the other ridges. All ridges are well developed. The soft seeds fit in the triangle-shaped depression. The crushing surface is flat in the cross section.

(B, H) Upper beak. The upper beak shows a very well developed morphology with clear ridges and depressions. Three ridges (yellow arrows) accompanied by two grooves run from the tip of the beak towards the posterior part. One of the grooves runs towards the middle, enlarges and ends at the medial elevation at the posterior end. The extension of the other groove extends and forms the deep round depression in the posterior part. The ridges and grooves run more or less parallel in the anterior three quarters of the beak. The posterior depressions (white/black arrow) are probably useful to keep the seed in place. A depression with an elevation on the midline forms the centre of the upper beak. All scale bars = 0.5 cm.

(C, D, I, J) Crushing surface morphology of the large morph. (C, I) Mandible. There is one weakly developed ridge which runs from the tip of the mandible in the anterior-posterior direction to the posterior end (red arrow). This ridge is situated at the middle of the crushing surface. The area close to the ridge is flat and nearly horizontal but becomes steeper towards the lingual and labial direction so that the crushing surface looks slightly rounded in the cross section. There is another ridge across the posterior end of the long anterior-posterior ridge with a width of 3-4 mm towards the labial direction (green arrow). After the 3-4 mm it bends under an angle of about 120° towards posterior. The short side-to-side ridge (blue arrow) runs also in the lingual direction, but only for 1-2 mm and bends posteriorly under a sub-perpendicular angle. These short ridges are probably there to resist forces while cracking the seeds rather than being involved in the actual cracking process.

(D, J) Upper beak. Two ridges (yellow arrows) accompanied by one groove run from the tip of the beak towards the posterior part. One ridge forms the outer, labial margin, the other ridge together with the groove extend and enlarge towards the posterior part and form the shallow, rounded and oval depression (white/black arrow). The ridges and the groove run

more or less parallel in the anterior half of the beak. A depression with an elevation on the midline and a high rectangle-shaped elevation at the posterior end forms the centre of the upper beak. There is an edge on each side on the outline of the beak halfway between the anterior and the posterior end; these edges are best to be seen in lateral view. All scale bars = 0.5 cm.

(E, F, K, L) Crushing surface morphology of the mega morph. (E, K) Mandible. The ridge, which runs from the tip of the beak to the posterior edge, is very weakly developed and runs along the middle of the crushing surface (red arrow). From this ridge a very rounded and strongly curved crushing surface originates in the lingual and labial direction in the posterior half of the mandible. The side-to-side ridge (blue arrow) that is situated at the posterior end of the anterio-posterior ridge is very well developed and about 4-5 mm wide. This short ridge extends smoothly towards the labial direction and under about 90° towards posterior at the lingual end. The well developed lingual-labial ridge might play a role in the cracking process, but its extensions are probably a support for resisting feeding induced forces.

(F, L) Upper beak. shows a highly flattened morphology; two ridges (yellow arrows) and one groove run from the tip towards the posterior end of the beak. The ridge on the labial side forms the outer margin of the beak, the other one bends towards the midline and continues in the middle posterior elevation. Both ridges are clearly apart from each other and do not run parallel. The groove extends to the wide, rounded and shallow depression (white/black arrow) in the posterior part of the beak. A shallow depression with a broad ridge over the midline and an elevated posterior rectangle is in the centre of the upper beak. All scale bars = 0.5 cm.

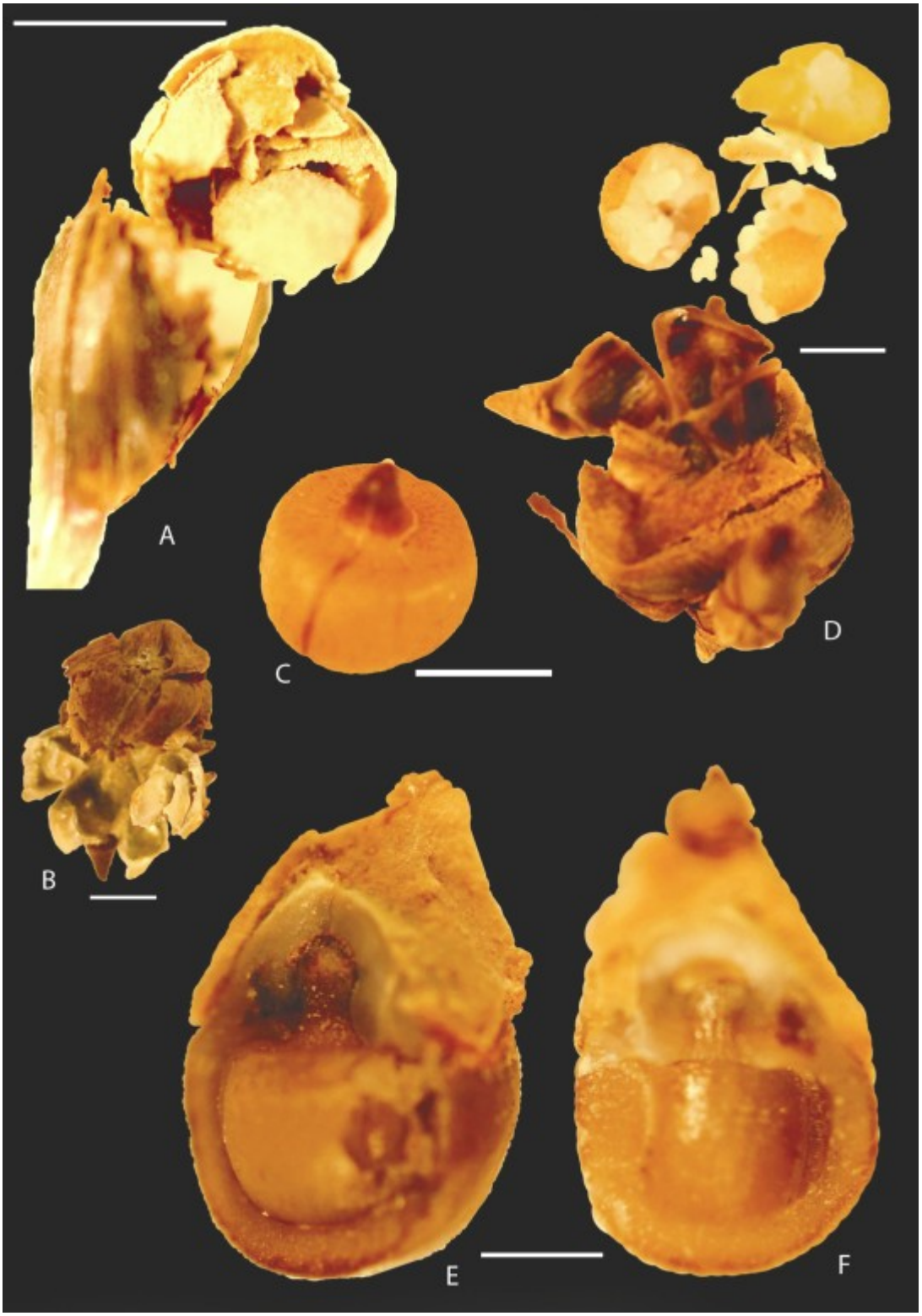

Figure S4. Examples of crushed seeds. (A) A smashed soft seed *Scleria goossensii*. (B) A cracked hard seed *Scleria verrucosa*. (C) A complete fruit of the very hard seed *Scleria racemosa*. (D) A crushed very hard seed resulting from cracking with the 5 mm-tool. (E, F) A very hard seed cracked with the three-point bending tool, cut in two halves and with the whole fruit preserved in the left half. All scale bars = 2 mm.

Table S1. The measurements of the mandibles of the three morphs in mm. Figure S1 shows" where the measurements were taken.

[mm]	small morph	large morph	mega morph
Total mandible width (TMW)	12.33	15.25	17.52
Inner mandible width (IMW)	3.64	2.71	3.10
Anterior crushing surface width (ACS)	2.94	3.51	4.05
Posterior crushing surface width (PCS)	3.32	5.00	6.02

Table S2

Click here to Download Table S2

Table S3

Click here to Download Table S3

Table S4

Click here to Download Table S4

Dataset 1

Click here to Download Dataset 1